Solid State Sciences 34 (2014) 56–62

Contents lists available at ScienceDirect

Solid State Sciences

journal homepage: www.elsevier.com/locate/ssscie

Thermoelectric properties of quaternary Uranium chalcogenides $Cs_2Pt_3US_6$ and $Cs_2Pt_3USe_6$

Fahad Ali Shah [a], Sikander Azam [b, *]

[a] Materials Modeling Lab, Department of Physics, Hazara University, Mansehra, Pakistan
[b] New Technologies – Research Center, University of West Bohemia, Univerzitni 8, 306 14 Pilsen, Czech Republic

ARTICLE INFO

Article history:
Received 30 March 2014
Received in revised form
20 May 2014
Accepted 22 May 2014
Available online 4 June 2014

Keywords:
Electronic structure
Fermi surface
Thermoelectric properties
DFT

ABSTRACT

Electronic and thermoelectric behaviors of $Cs_2Pt_3US_6$ and $Cs_2Pt_3USe_6$ compounds have been revealed in the present work. The calculations have been performed with the help of full potential linearized augmented plane wave method (FP-LAPW). Engel–Vosko generalize gradient approximation was used for the exchange correlation energy. Thermoelectric properties were deal with generalized BoltzTraP program. Band structure calculation resulted in metallic nature of the materials. Calculated Fermi surfaces have been found to consist of two sheets. Bonding characteristics have studied with the help of electron charge density in (1 1 0) crystallographic plane. Seebeck coefficient, electric conductivity, power factor, figure of merit and thermal conductivity has been calculated.

1. Introduction

Thermoelectric effects that have found in materials occur due to temperature difference between two dissimilar metals, create an electric potential and vice versa. Seebeck coefficient, Peltier effect and Thomson effect are such phenomena that are responsible for thermoelectric properties in the materials. Considerable attention has been given to thermoelectric materials due to their useful applications in electric generator, thermoelectric coolers, clean energy, photon sensing devises and mechanic free heat pump [1]. Materials selection criteria for thermoelectric are based on dimensionless quantity called figure of merit (ZT) [1,2].

$$ZT = \frac{S^2\sigma}{\kappa_e + \kappa_l}T$$

where S represents seebeck coefficient, σ is the electric conductivity, T is the absolute temperature and κ_e, κ_l are the thermal conductivities due electrons and lattice respectively. Above equation clearly shows that to obtain high figure of merit the material should have maximum value of seebeck coefficient and lower thermal conductivities of electrons and lattice. Materials that are under consideration and reported by researchers for thermoelectric device applications includes inorganic Clathrates [3], Half Heusler alloys [4], Complex oxides structured materials [5,6], transition metals Uranium chalcogenides [7] and Skutterudites thermoelectrics [8]. Present work has offered thermoelectric properties of two Quaternary Uranium Chalcogenides $A_2M_3UQ_6$ (A = Cs, M = Pt, Q = S, Se). These compounds were synthesized by reacting U, M and Q in ACl or A_2Q_x fluxes. The crystals of these compounds are of $NaBa_2Cu_3O_6$ structure type with space group *Fmmm* of the orthorhombic system. These structures are consists of hexagon formed from six edged M atoms which in turn edge shared with U atoms, forming layers among (0 1 0). Atoms 'A' separated these layers [7].

In this work, the full-potential linearized augmented plane-wave (FP-LAPW) method based on the density functional theory (DFT) with in the LDA, GGA and EVGGA exchange potential approximation is used to calculate accurately the electronic structure and electronic charge density of the $Cs_2Pt_3US_6$ and $Cs_2Pt_3USe_6$ compounds. We also calculated the thermoelectric properties for these materials. The rest of the paper has been divided in three parts. In Section2, we briefly describe the computational method used in this study. The most relevant results obtained for the electronic, electronic charge density of $Cs_2Pt_3US_6$ and $Cs_2Pt_3USe_6$ compounds are presented and discussed in Section3 we have discussed the thermoelectric properties. Finally, we summarize the main conclusions in Section5.

* Corresponding author. Tel.: +420 775928620.
E-mail addresses: sikander.physicst@gmail.com, sikandar_hu@yahoo.com (S. Azam).

http://dx.doi.org/10.1016/j.solidstatesciences.2014.05.009
1293-2558/

2. Methodology

Relevant quantities have been calculated using density functional theory (DFT) in the frame work of all electrons full potential linearize augmented plane wave (FP-LAPW) [9,10] method as implemented in WEIN2K suite of program [11]. In FP-LAPW method unit cell is split into atomic spheres (MT) and interstitials region (IR). The self-consistent calculations were said to be converged when the total energy difference of the crystal is 0.1 mRy and the total electronic charge difference is 0.001 e at which the structural geometry is relaxed. The exchange correlation potential has been treated with the help of Engel Vosko generalized gradient approximation (EVGGA) that is considered to be more superior to local density approximation (LDA) [12]. Due to the simplest nature of LDA and GGA that does not accurately reproduce the exchange-correlation energy and its charge derivatives. Such inability of these two approximations results in the underestimation of energy band gap [13]. This deficiency was fulfilled by Engel and Vosko by introducing new functional form of GGA called EVGGA [14]. Because EVGGA has adopted exchange-correlation potential V_{xC} as a functional instead of energy exchange E_{xC}, to give better splitting of the band structure

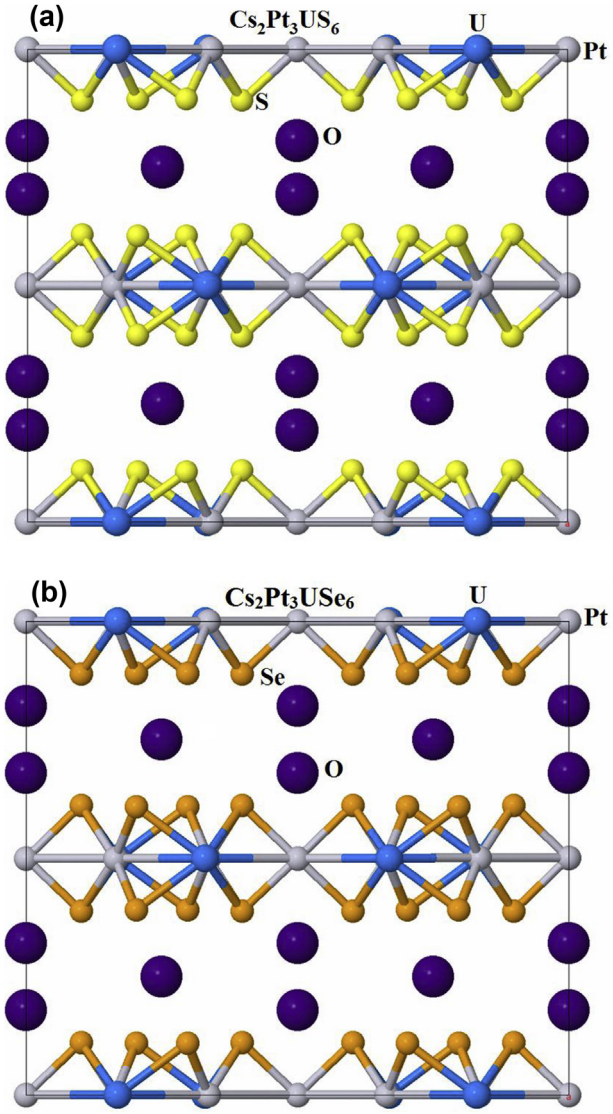

Fig. 1. Unit cells structure of (a) $Cs_2Pt_3US_6$ (b) $Cs_2Pt_3USe_6$.

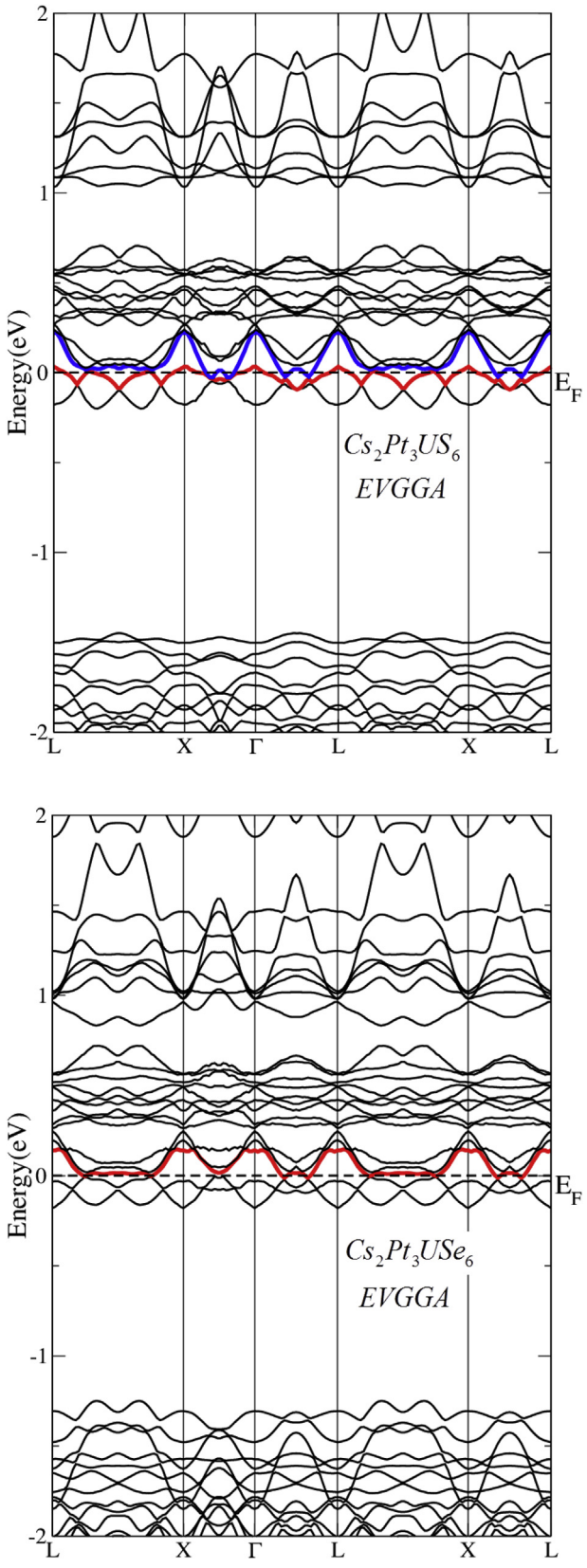

Fig. 2. Calculated band structures of $Cs_2Pt_3US_6$ and $Cs_2Pt_3USe_6$ compounds.

[15,16]. Crystal structures of both the compounds, $Cs_2Pt_3US_6$ and $Cs_2Pt_3USe_6$ have been shown in Fig. 1. Both the compounds have orthorhombic structural geometry with space group *Fmmm*. Lattice constants for $Cs_2Pt_3US_6$ are given as $a = 9.7924(8)$ Å, $b = 14.8937(8)$ Å, $c = 17.016(2)$ Å and for $Cs_2Pt_3USe_6$ are as follow $a = 10.0904(5)$ Å, $b = 15.3859(7)$ Å, $c = 17.5882(8)$ Å [17]. We have presented electronic band structure, density of states, surface charge density, Fermi surface and thermoelectric properties of the above mentioned compounds using FP-LAPW.

3. Results and discussion

3.1. Band structure and density of states

Energy band structure of $Cs_2Pt_3US_6$ and $Cs_2Pt_3USe_6$ compounds are shown in Fig. 2. The band structure calculations in case of both the compounds have carried out on the basis of optimized structures. The electronic band structure in case of above said compounds were calculated using EV-GGA by selecting high symmetry points. By close observation we noticed that valence and conduction band have crossed the Fermi energy level resulting in the metallic nature of both the compounds. Bonding nature, hybridization of states and contribution of orbitals to the electronic band structure all such aspects of the materials that can be clearly deduce from the total density (TDOS) and partial density of states (PDOS). TDOS and PDOS of $Cs_2Pt_3US_6$ and $Cs_2Pt_3USe_6$ compounds have been calculated using EVGGA scheme. The total and atom resolved partial density of states in a crystal cell is presented in Fig. 3 for the chosen compounds. Total density of states exhibits no change in the structure when replacing S atom by Se atom. The dominant state is Cs-p in the lower energies between −15 eV and −9 eV as compared to S—s and Se—s states. The peaks around Fermi level are from the

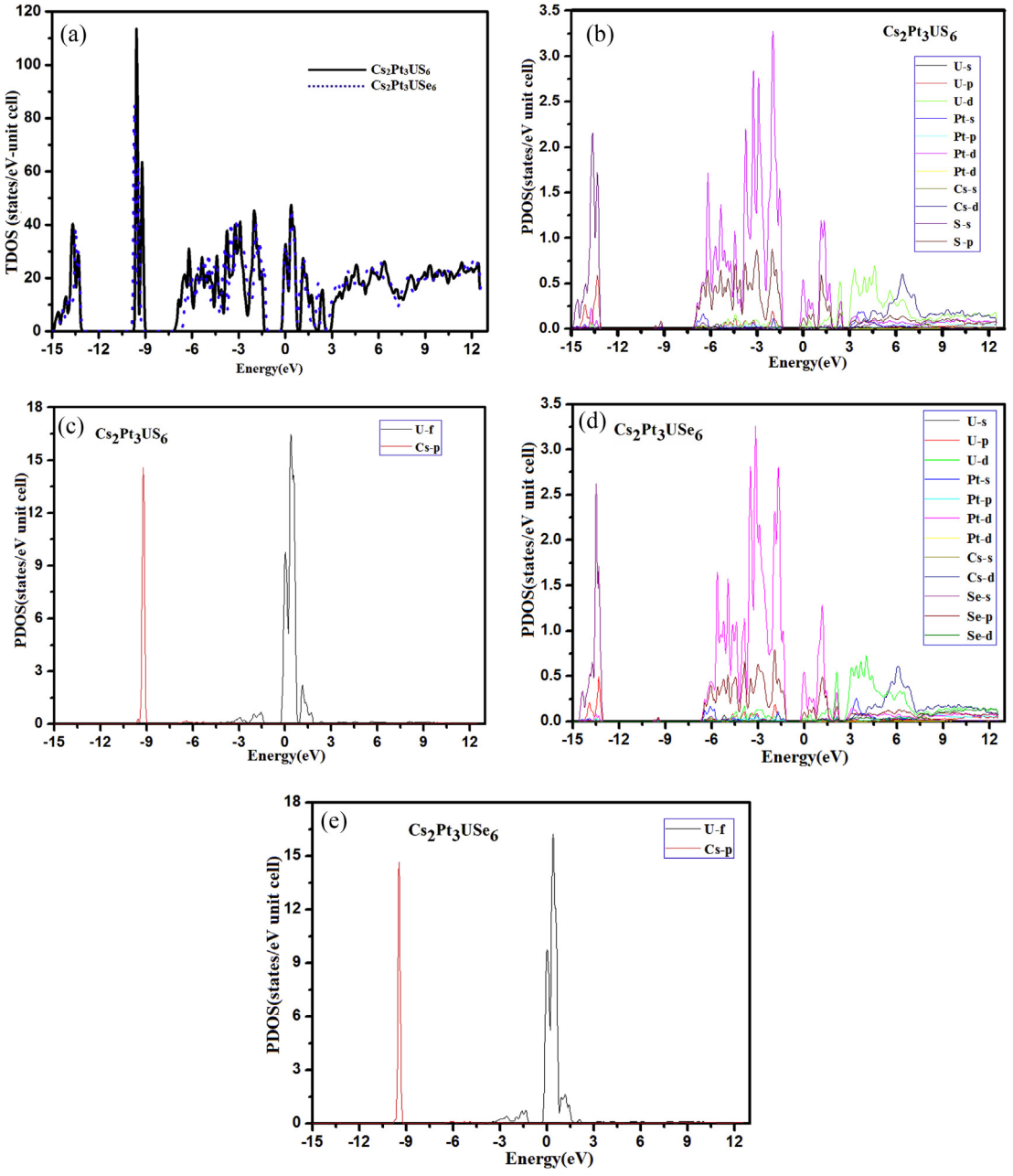

Fig. 3. Total density of states and partial density of states for $Cs_2Pt_3US_6$ and $Cs_2Pt_3USe_6$ compound.

participation of Pt-d, S-p, Se-p and U-d orbitals in which Pt-d has greater contribution to the structure. Weak hybridization is observed between Pt-p and Pt-s orbital in the extreme lower energies (−15 eV to −14 eV). In the higher energy region (0 eV–12 eV) structure is mostly dominated by U-f state while Cs-d and U-d states have very small contribution.

3.2. Electronic charge density

Contour plots of electron charge density are very helpful in predicting the chemical bonding and charge transfer in $Cs_2Pt_3US_6$ and $Cs_2Pt_3USe_6$ compounds. We have calculated the distribution of charge density for the investigated compounds in (1 1 0) crystallographic plane. The charge density contours plot in (1 1 0) plane can be seen in Fig. 4. Color scale represents the concentration of charges at the atomic sites from which we can easily identify maximum and minimum charge area around atoms. Zero charge area is indicated by the red color while maximum charge area is represented by blue color (in the web version). The S atoms share its valence electrons with U atoms and Pt atoms that give rise to covalent bond between these atoms. Since the electronegativity difference among S, U, Pt is very small which resulted in almost equal distribution of charge around these atoms. The same situation of charge transfer occurred by replacing S with Se as shown in the contours plots. Cs atoms in both the cases have occupied the region of zero charge density.

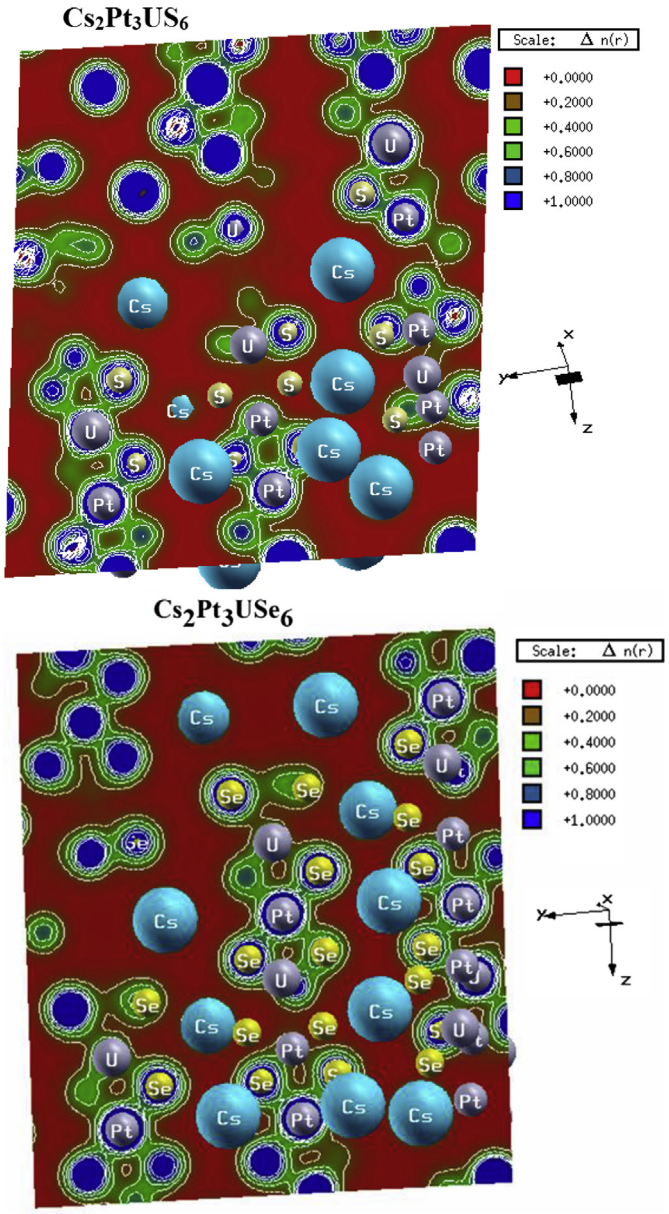

Fig. 4. Electronic charge density for $Cs_2Pt_3US_6$ and $Cs_2Pt_3USe_6$ compounds.

3.3. Fermi surface

Superconductivity mainly occurs due to the presence of electrons close to Fermi level. Electronic structure of metallic materials can be further explored with the help of Fermi surface (FS). In view of the fore-mentioned importance we have calculated the Fermi surfaces of $Cs_2Pt_3US_6$ and $Cs_2Pt_3USe_6$ compound. The calculated FS of these compounds using EVGGA scheme have been shown in Fig. 5. Conduction bands have crossed Fermi level that can easily be seen from band structure. De Haas Van Alphen (dHvA) experiment can be used to probe FS. In the present calculation two bands are found to cross the Fermi level in case of $Cs_2Pt_3US_6$ and $Cs_2Pt_3USe_6$ compound that give rise to two FS sheets. Band # 194 and 195 formed the Fermi surface of $Cs_2Pt_3US_6$ compound while band # 225 and band # 255 establish FS of $Cs_2Pt_3USe_6$. FS is composed of white spaces and colored regions representing holes and electrons respectively. The variation in the values of inter-atomic bonding, bond angles and degree of band filling attributed to different shapes of FS for both the compounds. The variation of color in FS is due to the change in velocity of electrons. In the FS plot red color designate those electrons that have maximum velocity while green color indicate that these electrons moves with moderate velocity (in the web version).

4. Thermoelectric properties

In the above section the purpose of reporting the comprehensive work on the electronic structure was to understand the band structure and density of states. It is clear that the aspect of band structure the thermoelectric properties are reasonably sensitive. Thus it is obvious that the consistency of the calculated thermoelectric properties would be dependent on the accurateness of the electronic structure calculations. As from the study of the electronic structure it is clear that our calculated compounds have the metallic nature. So in this section we have calculated the thermoelectric properties of the investigated compounds. As we know that the conversion of temperature gradient to voltage gradient is one the main advantage of thermoelectric materials. Thermoelectric materials have wide range of applications in power generation and refrigeration technologies [18–21]. Additional application in technological areas includes energy harvesting, smart sensors and newly developed concept of thermopower wave sources [22–26]. Metals possess crystalline structure and support heat flow when an external temperature is applied to it. Metals, similar to other solids materials, also possess a component of heat conduction called lattice (phonon) thermal conductivity k_l. Metals are unique due to the presence of free electrons as charge carriers. These charge carriers not only produce electric current but also account for the transport of heat. These charge carriers contribute mostly to the total thermal conductivity k_{tot} in case of metals. The contribution to the thermal conductivity is referred to as electronic thermal conductivity k_e. Therefore, heat current due to flow of electrons is far greater than the phonon contribution in case of metals. The electronic term is dominant and really should be taken under consideration to properly assess the heat conducting potential of metallic materials.

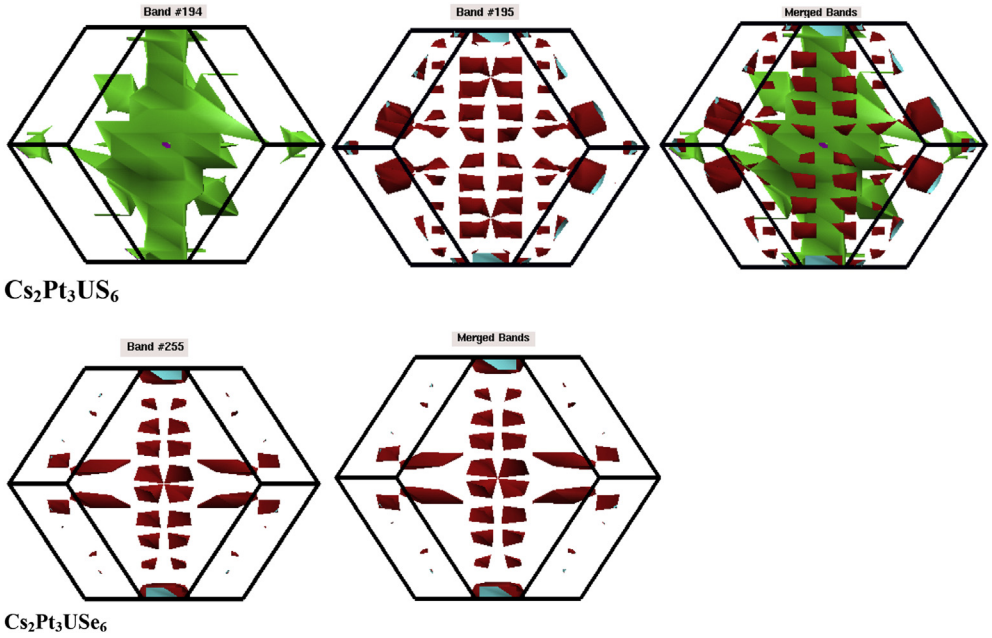

Fig. 5. Computed Fermi surfaces of $Cs_2Pt_3US_6$ and $Cs_2Pt_3USe_6$ compounds.

Calculated band structures shown in Fig. 2 help us to compute the transport properties of $Cs_2Pt_3US_6$ and $Cs_2Pt_3USe_6$ compound using the generalized BoltzTraP program and rigid band approximation [17]. In order to understand the thermoelectric behavior of the materials it is necessary to explore properties such as Seebeck coefficient S, electrical conductivity (σ), power factor ($S^2\sigma$) and thermal conductivity (k). A materials' electrical conductivity is due to the presence of free electrons. Providing thermal energy, excite the free electrons as a consequence the materials starts conduction. Calculated electrical conductivity σ of the investigated compounds has been shown in Fig. 6a. Electric conductivity has been plotted as a function of temperature on the horizontal axis. At room temperature i.e 300 K, $Cs_2Pt_3US_6$ and $Cs_2Pt_3USe_6$ compounds have maximum value of electric conductivity and at 600 K both compounds have shown same value of electric conductivity. As the temperature is raised both materials exhibited gradual decrease in the electrical conductivity but at higher temperature range, $Cs_2Pt_3US_6$ show a bit greater value of electrical conductivity than $Cs_2Pt_3USe_6$. Figure shows that both the materials have good electrical conductivity in the lower temperature range. As no experimentally or theoretically work has been found in literature who have calculated the thermoelectric properties for our calculated compounds so we compared our results with the work done by the ZHU et al. [27], with which our calculated work shows close agreement with there work. By heating thermocouples, electrons moves from warmer side towards colder region, electric field is setup due to the motion of these electrons. As a result a potential difference is created by the accumulation of electrons and holes on opposite sides. The ratio of voltage difference to temperature difference is Seebeck coefficient S. Seebeck coefficient determines how efficient a thermocouple is. We have presented seebeck coefficients for $Cs_2Pt_3US_6$ and $Cs_2Pt_3USe_6$ compound in Fig. 6b. Seebeck coefficient value for $Cs_2Pt_3USe_6$ has a maximum value in the middle of curve at around 550 K while for $Cs_2Pt_3US_6$ seebeck coefficient consistently increased in negative values as the temperature is increased. At 300 K, $Cs_2Pt_3USe_6$ has greater value of S (0.5×10^{-5} V/K) as compared to $Cs_2Pt_3US_6$ (-3.1×10^{-5} V/K). Negative seebeck coefficient indicated that dominating carriers are electrons. Our calculated results for the seebeck coefficient show the identical behavior with the experimental work of Melnyk et al. [28]. Usefulness of a thermoelectric material can be determine by yet another property, called power factor $P^{av} = S^2\sigma$. Power factor quantitatively measure the ability of materials to generate electric power. The calculated power factor for $Cs_2Pt_3US_6$ and $Cs_2Pt_3USe_6$ compounds are plotted in Fig. 6c. At 300 K, $Cs_2Pt_3USe_6$ material has obtained value of 0.1×10^9 W/mk^2 for P^{av} which slightly increased and then decreased till it reached to a minimum value at 800 K on the other hand $Cs_2Pt_3US_6$ attained P^{av} of approximately 1.1×10^{10} W/mk^2 at room temperature. Gradual increase in the power factor has been noticed from the graph as the temperature went up and reached to its maximum value of 4.6×10^{10} W/mk^2 at 800 K for $Cs_2Pt_3US_6$ compound. To gain further knowledge of thermoelectric properties of materials we decided to calculate temperature dependent thermal conductivity k. Thermal conductivity of materials is composed of electronic (k_e) and lattice (phonon) (k_l) contributions ($k = k_e + k_l$). The electronic portion is dominant and has greater contribution to the thermal conductivity. The calculated thermal conductivity of $Cs_2Pt_3US_6$ and $Cs_2Pt_3USe_6$ compounds has been presented in Fig. 6d At room temperature $Cs_2Pt_3US_6$ and $Cs_2Pt_3USe_6$ compounds have nonzero values of 9.4×10^{13} W/mks and 7.1×10^{13} W/mks respectively. Thermal conductivity increases with temperature for $Cs_2Pt_3US_6$ and $Cs_2Pt_3USe_6$ compounds and obtained a maximum value of 1.41×10^{14} W/mks and 9.7×10^{13} W/mks at 800 K respectively. $Cs_2Pt_3US_6$ has greater thermal conductivity as compared to $Cs_2Pt_3USe_6$ for the whole temperature values on scale. Figure of merit (ZT) determine the performance of thermoelectric materials. ZT bears direct relation with Seebeck coefficient and electric conductivity whereas inversely proportional to the thermal conductivity. Graphs of ZT for $Cs_2Pt_3US_6$ and $Cs_2Pt_3USe_6$ compounds are given in Fig. 6e. At room temperature $Cs_2Pt_3US_6$ and $Cs_2Pt_3USe_6$ have obtained ZT of 0.041 V/K and 0.002 V/K respectively. $Cs_2Pt_3US_6$ has attained maximum value of 0.266 V/K at 800 K while for $Cs_2Pt_3USe_6$ a value of 0.0017 V/K is calculated at 800 K. The maximum value for $Cs_2Pt_3USe_6$ is observed around 550 K on the graph.

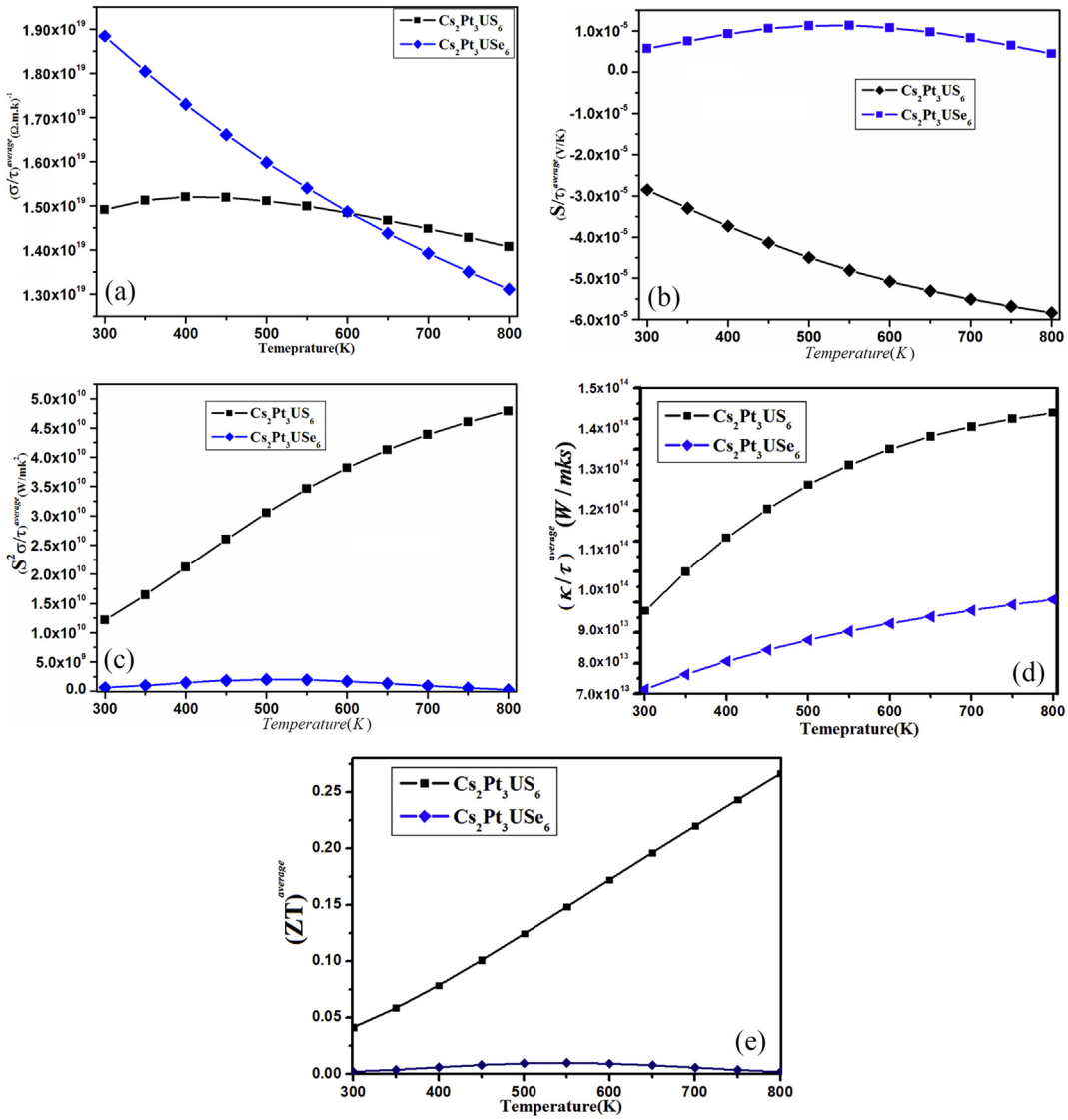

Fig. 6. Calculated (a) Electrical conductivity (b) Seebeck coefficient (c) Power factor (d) Thermalconductivity (e) Figure of merit.

5. Conclusion

All-electron full potential linearized augmented plane wave method based on density functional theory has applied to investigate the structural and electronic properties. Thermal properties are calculated using generalized BoltzTraP program. Band structure studied using EV-GGA help us to find that the materials are metallic in nature. Density of states showed that weak hybridization exists between Pt-p and Pt-s states (−15 eV to −14 eV). From charge density calculation it is found that S and Pt form covalent bond. Additionally, Cs has occupied region of minimum charge while maximum charge has accumulated around S atoms and Se atoms. Fermi surface is obtained and we concluded that they consist of two colored sheets for each compound ($Cs_2Pt_3USe_6$ and $Cs_2Pt_3US_6$). $Cs_2Pt_3USe_6$ compound has shown maximum electrical conductivity at room temperature. Seebeck coefficient of $Cs_2Pt_3US_6$ has hold up negative value which reflects that in $Cs_2Pt_3US_6$ maximum charge carriers are electrons. Further details about thermal properties have been extracted from power factor, figure of merit and thermal conductivity.

Acknowledgments

The result was developed within the CENTEM project, reg. no. CZ.1.05/2.1.00/03.0088, co-funded by the ERDF as part of the Ministry of Education, Youth and Sports (501100001823) OP RDI Programme.

References

[1] G.J. Snyder, E.S. Toberer, Nat. Mater. 7 (2008) 105.
[2] A.I. Hochbaum, R. Chen, R.D. Delgado, W. Liang, E.C. Garnett, M. Najarian, A. Majumdar, P. Yang, Nature 451 (2008) 2008.
[3] N.P. Blake, S. Latturner, J.D. Bryan, G.D. Stucky, H. Metiu, Band structures and thermoelectric properties of the clathrates $Ba_8Ga_{16}Ge_{30}$, $Sr_8Ga_{16}Ge_{30}$, $Ba_8Ga_{16}Si_{30}$, and $Ba_8In_{16}Sn_{30}$, J. Chem. Phys. 115 (2001) 8060–8064.
[4] Q. Shen, L. Chen, T. Goto, T. Hirai, J. Yang, G.P. Meisner, C. Uher, Effects of partial substitution of Ni by Pd on the thermoelectric properties of ZrNiSn-based half-Heusler compounds, Appl. Phys. Lett. 79 (2001) 4165–4167.
[5] I. Matsubara, R. Funahashi, T. Takeuchi, S. Sodeoka, T. Shimizu, K. Ueno, Fabrication of an all-oxide thermoelectric power generator, Appl. Phys. Lett. 78 (2001) 3627–3629.
[6] W. Shin, N. Murayama, K. Ikeda, S. Sago, Thermoelectric power generation using Li-doped NiO and (Ba, Sr)PbO_3 module, J. Power Sources 103 (2001) 80–85.

[7] George N. Oh, Eun Sang Choi, James A. Ibers, Inorg. Chem. 51 (2012) 4224–4230.
[8] H.A.R. Aliabad, M. Ghazanfari, I. Ahmad, M.A. Saeed, Ab initio calculations of structural, optical and thermoelectric properties for $CoSb_3$ and ACo_4Sb_{12} (A = La, Tl and Y) compounds, Comput. Mater. Sci. 65 (2012) 509–519.
[9] K.M. Wong, S.M. Alay-e-Abbas, A. Shaukat, Y. Fang, Y. Lei, J. Appl. Phys. 113 (2013) 014304.
[10] K.M. Wong, S.M. Alay-e-Abbas, Y. Fang, A. Shaukat, Y. Lei, J. Appl. Phys. 114 (2013) 034901.
[11] P. Blaha, K. Schwarz, G.K.H. Madsen, D. Kvasnicka, J. Luitz, WEIN2K, An Augmented Plane Wave + Local Orbitals Programme For Calculating Crystal Properties, Technische Universitat, Wein, Vienna, Austria, 2001, ISBN 3-9501031-1-2.
[12] F. Tran, P. Blaha, Phys. Rev. Lett. 102 (2009) 226401.
[13] P. Dufek, P. Blaha, K. Schwarz, Phys. Rev. B Condens. Matter Mater. Phys. 50 (1994) 7279.
[14] E. Engel, S.H. Vosko, Phys. Rev. B Condens. Matter Mater. Phys. 47 (1993) 13164.
[15] Z. Charifi, H. Baaziz, A.H. Reshak, Phys. Status Solidi B 244 (9) (2007) 3154.
[16] A.H. Reshak, Z. Charifi, H. Baaziz, Eur. Phys. J. B 60 (2007) 463.
[17] G.K.H. Madsen, D.J. Singh, Comput. Phys. Commun. 175 (2006) 67–71.
[18] H. Ohta, K. Sugiura, K. Koumoto, Recent progress in oxide thermoelectric materials: *p*-type $Ca_3CO_4O_9$ and *n*-type $SrTiO_3$, Inorg. Chem. 47 (2008) 8429–8436.
[19] K. Biswas, J.Q. He, I.D. Blum, C.I. Wu, T.P. Hogan, D.N. Seidman, et al., High-performance bulk thermoelectrics with all-scale hierarchical architectures, Nature 489 (2012) 414–418.
[20] H.J. Goldsmid, R.W. Douglas, The use of semiconductors in thermoelectric refrigeration, Br. J. Appl. Phys. 5 (1954) 386–390.
[21] T.M. Tritt, Thermoelectric phenomena, materials, and applications, in: D.R. Clarke, P. Fratzl (Eds.), Ann. Rev. Mater. Res. 412011, 2011, pp. 433–448.
[22] S. Walia, R. Weber, S. Balendhran, D. Yao, J.T. Abrahamson, S. Zhuiykov, et al., ZnO based thermopower wave sources, Chem. Commun. 48 (2012) 7462–7464.
[23] S. Walia, R. Weber, K. Latham, P. Petersen, J.T. Abrahamson, M.S. Strano, et al., Oscillatory thermopower waves based on Bi_2Te_3 films, Adv. Funct. Mater. 21 (2011) 2072–2079.
[24] S. Walia, R. Weber, S. Sriram, M. Bhaskaran, K. Latham, S. Zhuiykov, et al., Sb_2Te_3 and Bi_2Te_3 based thermopower wave sources, Energy Environ. Sci. 4 (2011) 3558–3564.
[25] S.B. Riffat, X.L. Ma, Thermoelectrics: a review of present and potential applications, Appl. Therm. Eng. 23 (2003) 913–935.
[26] S. Walia, S. Balendhran, P. Yi, D. Yao, S. Zhuiykov, M. Pannirselvam, et al., MnO_2 based thermopower wave sources with exceptionally large output voltages, J. Phys. Chem. C. 117 (2013) 9137–9142.
[27] T.J. Zhu, C. Yu, J. He, S.N. Zhang, X.B. Zhao, Terry M. Tritt, J. Electron. Mater. 38 (2009) 1068.
[28] G. Melnyk, E. Bauer, P. Rogl, R. Skolozdr, E. Seidl, J. Alloys Compd. 296 (2000) 235–242.